nature photonics

LETTERS

PUBLISHED ONLINE: 7 JULY 2013 | DOI: 10.1038/NPHOTON.2013.172

Entanglement-enhanced detection of single-photon scattering events

C. Hempel[1,2], B. P. Lanyon[1], P. Jurcevic[1,2], R. Gerritsma[1†], R. Blatt[1,2] and C. F. Roos[1,2*]

The ability to detect the interaction of light and matter at the single-particle level is becoming increasingly important for many areas of science and technology. The absorption or emission of a photon on a narrow transition of a trapped ion can be detected with near unit probability[1,2], thereby enabling the realization of ultra-precise ion clocks[3,4] and quantum information processing applications[5]. Extending this sensitivity to broad transitions is challenging due to the difficulty of detecting the rapid photon scattering events in this case. Here, we demonstrate a technique to detect the scattering of a single photon on a broad optical transition with high sensitivity. Our approach is to use an entangled state to amplify the tiny momentum kick an ion receives upon scattering a photon. The method should find applications in spectroscopy of atomic and molecular ions[6–9] and quantum information processing.

An ion in an electric trap provides an excellent system for carrying out precision spectroscopy. Laser cooling[10], either directly or sympathetically via an auxiliary ion[11], minimizes thermal line broadening. Long storage times allow for many repeated measurements on the same particle, and collisional shifts are non-existent. A key requirement is to detect whether photons of a given frequency of light are scattered. For some narrow ionic transitions, corresponding to long excited-state lifetimes, the electronic configuration change associated with photon absorption or emission can be detected with near 100% efficiency using the electron shelving technique[1]. In the general case where electron shelving cannot be implemented directly on a 'spectroscopy' ion of interest, efficient detection is possible using a co-trapped auxiliary 'logic' ion following the technique of quantum logic spectroscopy[12]. Here, information about the electronic state of the spectroscopy ion is mapped via a joint vibrational mode to the electronic state of the logic ion, where it can be read out. Alternatively, state mapping can be accomplished via an off-resonantly induced optical dipole force exciting the vibrational mode conditional on the state of the spectroscopy ion[13]. For broad transitions, quantum logic spectroscopy fails due to the extremely short excited-state lifetimes and the resulting inability to spectrally resolve their vibrational sidebands[2].

Another signature of a photon scattering event is the recoil kick an ion receives upon absorbing or emitting a photon[14]. The size of the recoil can be characterized by the ratio of the recoil energy E_{rec} to the energy of a quantum of motion $h\nu$ of a harmonically trapped ion oscillating at frequency ν, in the form of the dimensionless Lamb–Dicke factor $\eta = \sqrt{E_{\mathrm{rec}}/(h\nu)}$. For experiments on optical transitions, the Lamb–Dicke factor typically satisfies $\eta \ll 1$. For an ion cooled to its motional ground state, the probability of being promoted to the next higher vibrationally excited state by the recoil of an absorbed photon is η^2. Consequently, the method of monitoring the ground-state population is inefficient for detecting absorption events. Spectral lines from broad transitions have been reconstructed by observing changes in the fluorescence of a laser-cooled control ion via scattering of many hundreds of photons[15].

We now describe a technique for amplifying the recoil signal of single photons, which is independent of the particular spectroscopic ion species of interest (Fig. 1). As with quantum logic spectroscopy, a co-trapped logic ion encodes a two-level qubit with ground and excited states $|\downarrow\rangle_z$ and $|\uparrow\rangle_z$, respectively. The logic qubit and a common vibrational mode of the two-ion crystal are prepared in their respective ground states. A state-dependent force applied to this mode splits the vibrational state into two parts, each correlated with a different eigenstate in the logic qubit[16,17]. Consequently, logic qubit and motional state become entangled into a Schrödinger cat state of the form $\Psi = (|\rightarrow\rangle_x|+\alpha\rangle + |\leftarrow\rangle_x|-\alpha\rangle)/\sqrt{2}$, where $|\rightarrow\rangle_x$ and $|\leftarrow\rangle_x$ are eigenstates of the σ_x Pauli operator and $|\pm\alpha\rangle$ are coherently displaced motional states.

In the next step, spectroscopy light of a known frequency is sent into the trap. The inverse cat generation operation is then applied, thereby recombining the two vibrational components of the cat state and disentangling them from the logic qubit. If no spectroscopy photon is absorbed, the initial state of the logic qubit $|\downarrow\rangle_z$ is recovered. Otherwise, the recoil of the spectroscopy ion causes both vibrational components to be displaced by η_{abs} so that after recombination the total path in phase space encloses an area. Here, η_{abs} denotes the Lamb–Dicke factor of the absorbing transition. The result is a geometric phase[18] $\phi_{\mathrm{abs}} = 2\alpha\eta_{\mathrm{abs}}\sin\varphi_{\mathrm{sc}}$, proportional to the cat state size α and the photon recoil momentum, which leaves the final logic qubit state rotated by $\exp(\mathrm{i}\phi_{\mathrm{abs}}\sigma_x)$[19,20]. Here, $\varphi_{\mathrm{sc}} = 2\pi\nu\tau$ is the scatter phase, where τ is the time delay between photon absorption and the time of the largest spatial extent of Ψ oscillating at frequency ν. Measurements of the logic qubit spin projections $\langle\sigma_z\rangle = -\cos(\phi_{\mathrm{abs}})$ or $\langle\sigma_y\rangle = \sin(\phi_{\mathrm{abs}})$, using standard electron shelving for example, provide information about the photon absorption process. In summary, the small recoil displacement of the spectroscopy ion is converted into a large geometric phase and mapped onto the logic qubit's electronic state.

A complete photon scattering event involves two momentum kicks—one in absorption and one in emission. Because the absorbed photon comes from a directed laser beam, ideally this beam points parallel to the vibrational mode supporting the cat state. The recoil direction due to the spontaneously emitted photon is random. The effect is to add a second, random geometric phase $\phi_{\mathrm{em}} = \tilde{\phi}_{\mathrm{em}}\cos\theta$ to the measured signal $\langle\sigma_z\rangle = -\overline{\cos(\phi_{\mathrm{abs}} + \phi_{\mathrm{em}})}$, where the bar indicates averaging over the random photon emission angle θ with respect to the orientiation of the cat state in space, and $\tilde{\phi}_{\mathrm{em}} = 2\alpha\eta_{\mathrm{em}}\sin\varphi_{\mathrm{sc}}$. For an isotropic emission pattern, this expression reduces to

[1]Institut für Quantenoptik und Quanteninformation, Österreichische Akademie der Wissenschaften, Technikerstr. 21a, 6020 Innsbruck, Austria, [2]Institut für Experimentalphysik, Universität Innsbruck, Technikerstr. 25, 6020 Innsbruck, Austria; [†]Present address: QUANTUM, Institut für Physik, Universität Mainz, Staudingerweg 7, 55128 Mainz, Germany. *e-mail: christian.roos@oeaw.ac.at

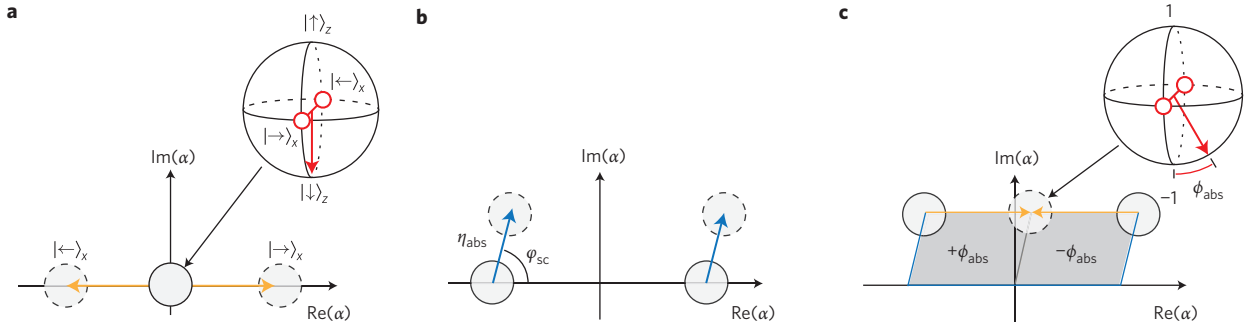

Figure 1 | Cat-state spectroscopy in phase space. a, Schrödinger cat state preparation. A qubit encoded in a logic ion, initialized in $|\downarrow\rangle_z$ (inset Bloch sphere), becomes entangled with a joint vibrational mode of the two-ion crystal formed with the co-trapped spectroscopy ion. **b**, Absorption of a photon by the spectroscopy ion causes a displacement of size η_{abs} (magnified for clarity) in a direction determined by the event's timing φ_{sc} relative to the oscillation of the cat state. **c**, The cat state is re-interfered, disentangling the internal state from the motion and leaving the geometric phase ϕ_{abs} in the logic ion's internal state, where it can be read out via standard electron shelving.

$$\langle\sigma_z\rangle = -\cos(\phi_{abs})\mathrm{sinc}(\tilde{\phi}_{em}) \quad (1)$$

and similarly $\langle\sigma_y\rangle = \sin(\phi_{abs})\mathrm{sinc}(\tilde{\phi}_{em})$.

In our demonstration we confine a mixed-species two-ion crystal in a linear Paul trap (see Methods). The isotopes $^{40}Ca^+$ and $^{44}Ca^+$ are used as logic and spectroscopy ions, respectively (Fig. 2a). The $^{40}Ca^+$ provides sympathetic Doppler and vibrational ground-state cooling of the lowest-frequency axial vibrational mode at $\nu = 1.199$ MHz, a narrow electronic transition in which to encode a qubit ($S_{1/2} \rightarrow D_{5/2}$) and qubit state readout via electron shelving. We optically pump $^{44}Ca^+$ to its metastable $D_{3/2}$ state to perform spectroscopy on the strong $D_{3/2} \rightarrow P_{1/2}$ open dipole transition. Absorption of a single infrared photon populates the $P_{1/2}$ state (lifetime of 7.1 ns; ref. 21), which—with 96.6% probability[22]—will decay to the $S_{1/2}$ ground state under emission of a single blue photon. The experimental sequence is presented in Fig. 2b. A state-dependent force[23] is realized using a bichromatic laser field resonant with the red ($-\nu$) and blue ($+\nu$) vibrational sidebands of the logic qubit. A train of short (~60 ns) spectroscopy pulses, separated by $1/\nu$, is shifted in time by τ to vary φ_{sc} in order to retrieve the fringe pattern shown in Fig. 3a for a cat state size of $\alpha = 2.9(2)$. Precise timing of photon absorption is critical for the measurement of $\langle\sigma_y\rangle$. A discussion of timing issues and data for other values of α is presented in Supplementary Sections S2 and S5. Because the signal $\langle\sigma_z\rangle$ (blue curve) is insensitive to the sign of the geometric phase shift, the fringe period is equal to half the motional period. Conversely, signal $\langle\sigma_y\rangle$ (red curve) is sign-sensitive and therefore oscillates around 0 with a period equal to the motional period $1/\nu$. Furthermore, while the signal in $\langle\sigma_z\rangle$ is sensitive to the recoils of absorbed and re-emitted photon, the signal in $\langle\sigma_y\rangle$ is predominantly due to the recoil of the absorbed photon in the limit of small geometric phases as it depends on ϕ_{abs} in first order and on ϕ_{em} in second order.

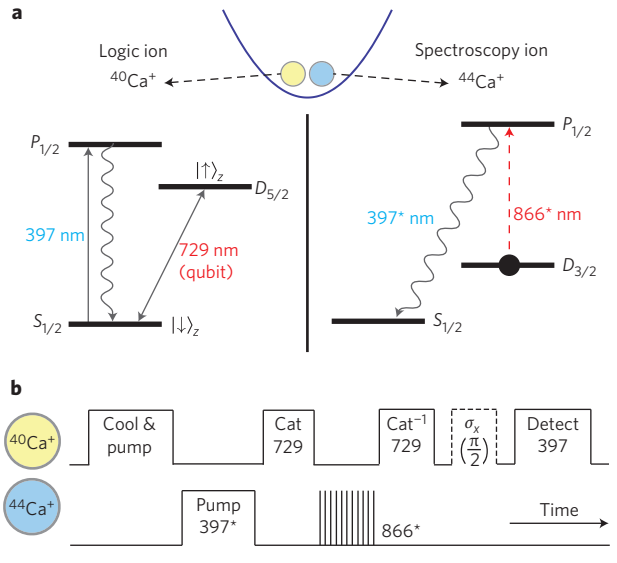

Figure 2 | Experimental details. a, Relevant electronic energy levels. **b**, Experimental laser pulse sequence. The $^{40}Ca^+$ dipole transition at 397 nm is used for laser cooling, optical pumping and state detection of the optical qubit implemented on its 729 nm narrow quadrupole transition, which is also used for ground-state cooling of the joint vibrational mode. The asterisk indicates isotope shifts[26] that allow off-resonant scattering from the respective other isotope to be safely ignored at the light intensities used. Dedicated laser beams resonant with the $^{44}Ca^+$ transitions are used for initialization (397* nm) and spectroscopy (866* nm pulse train).

A line profile of the single-photon transition in $^{44}Ca^+$ was recovered using the cat state technique (Fig. 3b). The $\langle\sigma_y\rangle$ signal amplitude was measured as a function of the spectroscopy laser frequency at a reduced light intensity. The observed linewidth of 38(5) MHz is close to the width expected due to the combination of the transition's natural linewidth (22.4 MHz) with the Zeeman splitting caused by an applied magnetic field of 4 gauss. We wish to emphasize that this profile is due, with high probability, to at most a single infrared photon scattering on an open dipole transition.

The uncertainty in the spectroscopic signal is determined by quantum projection noise[24] in estimating the expectation values of the logic qubit state. The signal-to-noise ratio (SNR) can always be increased by taking more measurements. To compare different methods it is therefore useful to renormalize by the number of measurements (N) made and consider the sensitivity $\beta = \mathrm{SNR}/\sqrt{N}$ provided by each method. For comparison we implemented two additional direct detection schemes that do not exploit a non-classical state to amplify the scattering signal. The first and most basic of the two schemes directly measures the probability of the motional state being excited from $|0\rangle$ to $|1\rangle$ (phonons) in a single-photon scattering event by applying a red-sideband π pulse to the logic ion followed by a measurement of $\langle\sigma_z\rangle$. In the second scheme, $\langle\sigma_y\rangle$ is measured instead. Here, phase-sensitive detection of the motional state is enabled by keeping the pulse envelope of the spectroscopy laser phase-locked to the beat signal (at frequency 2ν) of the two laser fields manipulating the ions' motion (Supplementary Section S1).

Table 1 summarizes the experimentally determined sensitivities. Compared to the direct detection method, cat-state spectroscopy

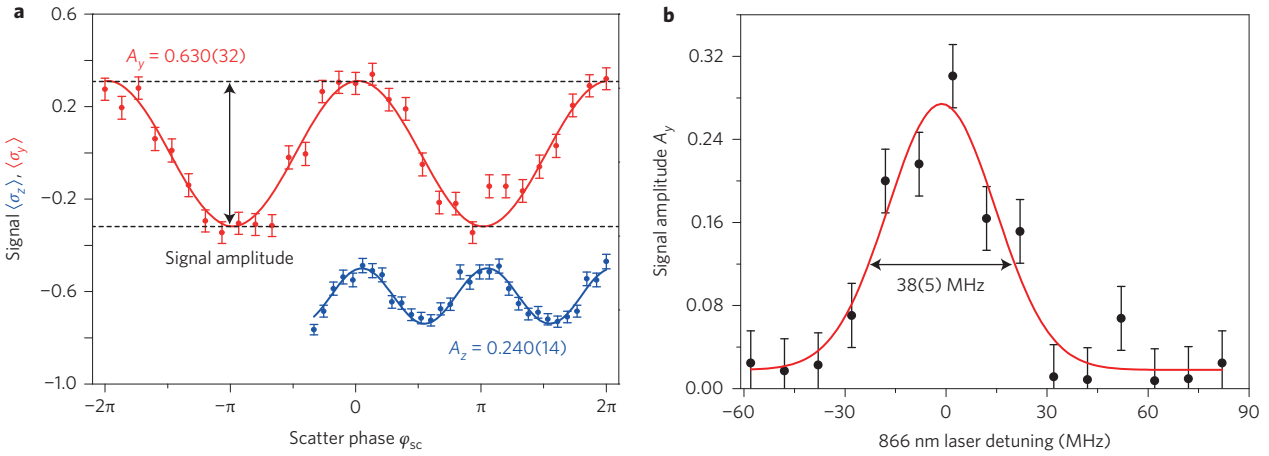

Figure 3 | Cat-state spectroscopy results. Photon scattering signals on the broad $D_{3/2} \rightarrow P_{1/2}$ transition in $^{44}Ca^+$ for a cat state size of $\alpha = 2.9(2)$. **a**, Interferometic fringes observed by varying φ_{sc} (the relative timing) of a single-photon scattering event with respect to the cat-state oscillation phase. Weighted sinusoidal fits (solid lines) yield a signal amplitude A in the two detection bases σ_z (blue curve) and σ_y (red curve). To maximize the contrast for the cat state size used, the data are taken at light intensities that ensure a complete pump-out of the $D_{3/2}$ level, such that with 93.6% probability a single (6.4% probability ≥ 2) photon is being scattered. **b**, Line profile of the transition taken in the σ_y detection basis. At each spectroscopy laser frequency, A_y is measured by alternating between the maximum and minimum of the fringe pattern. To avoid power broadening, the light level was reduced significantly, yielding a smaller signal amplitude as, even on resonance, it is not the case that in all experiments a photon is being scattered (Supplementary Section S6). All error bars are calculated from quantum projection noise.

using a cat state of $\alpha = 2.9(2)$ enabled an 18-fold improvement in measurement sensitivity. Also presented are results showing that, unlike the direct detection methods, cat-state spectroscopy even works without ground-state cooling. Theoretically, the method should work as well with thermal states that lie within the Lamb–Dicke regime, which can be reached with standard Doppler cooling[25]. Experimentally, a loss in contrast is seen, the origin of which requires additional study.

In principle, the technique's sensitivity can be further enhanced by making larger cat states. However, experimental errors will limit the useful cat size and therefore the achievable sensitivity. In our experiment, the dominant error source is electric field noise on the trap electrodes, which adds another random geometric phase ϕ_h. As a result, the contrast of the signal given in equation (1) needs to be multiplied by a factor $\exp(-\phi_h^2/2)$ with $\phi_h^2 = 8R_h n_{cat}\left(\frac{2}{3}\tau_{cat} + \tau_{wait}\right)$ where R_h is the mode's heating rate, $n_{cat} = |\alpha|^2$ the cat-state size in phonons, τ_{cat} the time needed for creating the cat state, and τ_{wait} the time between cat creation and recombination (Methods and Supplementary Section S4). The larger the cat state, the more detrimental the noise becomes. For the $\langle\sigma_y\rangle$ measurement in Fig. 3a and the experimental parameters $n_{cat} = 8.3(1.0)$, $\tau_{cat} = 50(2)\ \mu s$, $\tau_{wait} = 32(2)\ \mu s$, $R_h = 40(20)\ s^{-1}$, we expect a contrast reduction factor of 0.91(5) and an overall signal amplitude of $A_y = 0.54(4)$, which is close to the observed value.

Table 1 | Comparison of spectroscopic techniques.

Method	Sensitivity (β)	Measurements to reach 3σ
Direct detection $\langle\sigma_z\rangle$	0.018(6)	$2.7(1.9) \times 10^5$
Phase-sensitive $\langle\sigma_y\rangle$ direct detection	0.107(10)	$7.8(1.5) \times 10^2$
CSS $\langle\sigma_z\rangle$-signal	0.162(16)	$3.4(0.6) \times 10^2$
CSS $\langle\sigma_y\rangle$-signal	0.338(16)	$7.9(0.8) \times 10^1$
CSS $\langle\sigma_y\rangle$-signal*	0.109(14)	$7.6(2.0) \times 10^2$

The sensitivity of various cat-state spectroscopy (CSS) techniques using $\alpha = 2.9(2)$, and those that do not use a non-classical state, are compared (see main text). Also given are the number of measurements required to reach a confidence of three standard deviations (σ) in the detection of a scattering event. All errors are calculated from quantum projection noise.
*The result for a CSS measurement without ground-state cooling.

We have demonstrated a method for detecting light scattering from broad ionic transitions at the single-photon level. Complementing quantum logic spectroscopy for narrow transitions, cat-state spectroscopy should provide access to a new range of atomic and molecular ion transitions for precision spectroscopy. Fundamentally, the method can approach deterministic single-photon scattering detection. Assuming that the absorbed and emitted photons have the same wavelength, equation (1) gives the maximum probability of detecting a scattering event, in a single measurement, as 61%. The limit, imposed by the random emission direction of the emitted photon, could be overcome by using multiple vibrational modes or by modifying the emission direction, for example by the introduction of a cavity. In our experiment, the achieved sensitivity could be boosted significantly by using an ion trap with a reduced heating rate.

A deterministic measurement of whether an ion has scattered a photon would be of interest to the field of quantum information processing, especially as this measurement could be non-destructive with respect to the joint ion–photon state.

Methods

Experimental set-up. The experiments made use of a linear Paul trap with a minimal ion–electrode distance of 565 μm. Ions were loaded by isotope-selective photoionization from a resistively heated oven. The bichromatic laser beam used to create and re-interfere the cat state was generated by applying two radiofrequencies offset by 2ν to a single acousto-optic modulator, effectively producing a beat note to which the generator producing the pulse train of spectroscopy light was locked.

Geometric phases contributing to the spectroscopic signal. The total geometric phase that rotates the logic qubit state is given by $\phi = \phi_{abs} + \phi_{em} + \phi_h$, in which the terms arise from photon absorption and emission recoil, and random electric fields displacing the ions, respectively. In contrast to the deterministic phase ϕ_{abs}, the other two phases are independent random variables with vanishing odd-order moments. This property simplifies the calculation of expectation values at the end of the spectroscopy protocol, leading to $\langle\sigma_z\rangle = -\overline{\cos(\phi_{abs} + \phi_{em} + \phi_h)} = \cos(\phi_{abs})\overline{\cos\phi_{em}}\,\overline{\cos\phi_h}$ and $\langle\sigma_y\rangle = \overline{\sin(\phi_{abs} + \phi_{em} + \phi_h)} = \sin(\phi_{abs})\overline{\cos\phi_{em}}\,\overline{\cos\phi_h}$.

As spontaneous emission from the $P_{1/2}$ to $S_{1/2}$ state is isotropic, $\overline{\cos\phi_{em}} = \frac{1}{2}\int_0^\pi d\theta \sin\theta \cos(\tilde{\phi}_{em}\cos\theta)$. Writing the integrand as a Taylor series and carrying out the integration results in the sinc-function appearing in equation (1).

Electric field noise at the trap electrodes with frequencies close to the vibrational mode supporting the cat state leads to displacements of the motional state in random

directions. White noise acting on a cat of size n_{cat} for a duration τ adds a random geometric phase ϕ_h with zero mean and a variance given by $\overline{\phi_h^2} = 8R_h n_{cat}\tau$ (ref. 19). In our model, we assume noise acting on the state throughout the experimental steps of cat-state creation, photon scattering and cat recombination, where the steps last for times τ_{cat}, τ_{wait} and τ_{cat}, respectively. If a spin-dependent force of constant amplitude is used for cat creation and recombination, we have to make the replacement $\tau \rightarrow \frac{1}{3}2\tau_{cat} + \tau_{wait}$ where the factor $1/3$ accounts for the smaller average cat size during the first and last steps (Supplementary Section S4).

Received 16 January 2013; accepted 31 May 2013; published online 7 July 2013

References

1. Dehmelt, H. G. Mono-ion oscillator as potential ultimate laser frequency standard. *IEEE Trans. Instrum. Meas.* **31,** 83–87 (1982).
2. Leibfried, D., Blatt, R., Monroe, C. & Wineland, D. Quantum dynamics of single trapped ions. *Rev. Mod. Phys.* **75,** 281–324 (2003).
3. Rosenband, T. *et al.* Frequency ratio of Al^+ and Hg^+ single-ion optical clocks; metrology at the 17th decimal place. *Science* **319,** 1808–1812 (2008).
4. Chou, C., Hume, D., Koelemeij, J., Wineland, D. & Rosenband, T. Frequency comparison of two high-accuracy Al^+ optical clocks. *Phys. Rev. Lett.* **104,** 070802 (2010).
5. Häffner, H., Roos, C. F. & Blatt, R. Quantum computing with trapped ions. *Phys. Rep.* **469,** 155–203 (2008).
6. Nguyen, J. H. V. *et al.* Challenges of laser-cooling molecular ions. *New J. Phys.* **13,** 063023 (2011).
7. Mur-Petit, J. *et al.* Temperature-independent quantum logic for molecular spectroscopy. *Phys. Rev. A* **85,** 022308 (2012).
8. Leibfried, D. Quantum state preparation and control of single molecular ions. *New J. Phys.* **14,** 023029 (2012).
9. Ding, S. & Matsukevich, D. N. Quantum logic for the control and manipulation of molecular ions using a frequency comb. *New J. Phys.* **14,** 023028 (2012).
10. Wineland, D. J. & Itano, W. M. Laser cooling of atoms. *Phys. Rev. A* **20,** 1521–1540 (1979).
11. Larson, D. J., Bergquist, J. C., Bollinger, J. J., Itano, W. M. & Wineland, D. J. Sympathetic cooling of trapped ions: a laser-cooled two-species nonneutral ion plasma. *Phys. Rev. Lett.* **57,** 70–73 (1986).
12. Schmidt, P. O. *et al.* Spectroscopy using quantum logic. *Science* **309,** 749–752 (2005).
13. Hume, D. B. *et al.* Trapped-ion state detection through coherent motion. *Phys. Rev. Lett.* **107,** 243902 (2011).
14. Weiss, D. S., Young, B. C. & Chu, S. Precision measurement of the photon recoil of an atom using atomic interferometry. *Phys. Rev. Lett.* **70,** 2706–2709 (1993).
15. Clark, C. R., Goeders, J. E., Dodia, Y. K., Viteri, C. R. & Brown, K. R. Detection of single-ion spectra by Coulomb-crystal heating. *Phys. Rev. A* **81,** 043428 (2010).
16. Poyatos, J. F., Cirac, J. I., Blatt, R. & Zoller, P. Trapped ions in the strong-excitation regime: ion interferometry and nonclassical states. *Phys. Rev. A* **54,** 1532–1540 (1996).
17. Monroe, C. R., Meekhof, D. M., King, B. E. & Wineland, D. J. A 'Schrodinger cat' superposition state of an atom. *Science* **272,** 1131–1136 (1996).
18. Chaturvedi, S., Sriram, M. S. & Srinivasan, V. Berry's phase for coherent states. *J. Phys. A* **20,** L1071–L1075 (1987).
19. Turchette, Q. A. *et al.* Decoherence and decay of motional quantum states of a trapped atom coupled to engineered reservoirs. *Phys. Rev. A* **62,** 053807 (2000).
20. Munro, W. J., Nemoto, K., Milburn, G. J. & Braunstein, S. L. Weak-force detection with superposed coherent states. *Phys. Rev. A* **66,** 023819 (2002).
21. Jin, J. & Church, D. A. Precision lifetimes for the Ca^+ $4p\ ^2P$ levels: experiment challenges theory at the 1% level. *Phys. Rev. Lett.* **70,** 3213–3216 (1993).
22. Ramm, M., Pruttivarasin, T., Kokish, M., Talukdar, I. & Häffner, H. Precision measurement method for branching fractions of excited $P_{1/2}$ states applied to $^{40}Ca^+$. Preprint at http://arxiv.org/abs/1305.0858v1 (2013).
23. Haljan, P. C., Brickman, K-A., Deslauriers, L., Lee, P. J. & Monroe, C. Spin-dependent forces on trapped ions for phase-stable quantum gates and entangled states of spin and motion. *Phys. Rev. Lett.* **94,** 153602 (2005).
24. Itano, W. M. *et al.* Quantum projection noise: population fluctuations in two-level systems. *Phys. Rev. A* **47,** 3554–3570 (1993).
25. Kirchmair, G. *et al.* Deterministic entanglement of ions in thermal states of motion. *New J. Phys.* **11,** 023002 (2009).
26. Lucas, D. M. *et al.* Isotope-selective photoionization for calcium ion trapping. *Phys. Rev. A* **69,** 012711 (2004).

Acknowledgements

This work was supported by the European Commission via the integrated project Atomic QUantum TEchnologies and a Marie Curie International Incoming Fellowship.

Author contributions

C.R. conceived and designed the experiments. C.H., B.L., P.J., R.G. and C.R. performed the experiments. C.H., B.L. and C.R. analysed the data. C.H., B.L., R.G., R.B. and C.R. contributed materials and analysis tools. C.H., B.L. and C.R. wrote the paper.

Additional information

Supplementary information is available in the online version of the paper. Reprints and permissions information is available online at www.nature.com/reprints. Correspondence and requests for materials should be addressed to C.F.R.

Competing financial interests

The authors declare no competing financial interests.